J. Fluid Mech. (1980), *vol.* 100, *part* 2, *pp.* 349–365
Printed in Great Britain

Diffusion mixing in grid turbulence without mean shear

By BARRY GILBERT

Research Department, Grumman Aerospace Corporation, Bethpage, New York 11714

(Received 18 October 1978 and in revised form 17 January 1980)

An experimental examination of the fundamental properties of free turbulent interactions in a mixing flow has been conducted. A turbulent, two-dimensional, incompressible, uniform-density mixing layer was produced by using a parallel bar grid of different bar spacings but the same space to bar diameter ratio $M/D = 2$. In this unique mixing-flow geometry, two initially parallel flowing streams of air were formed in such a way as to possess the same mean structure but different turbulent kinetic energy. The mixing phenomenon was driven solely by the turbulent kinetic-energy self-diffusion process.

The data showed the development of the turbulent properties without the interference caused by turbulence generated by a mean shear flow. A simple diffusion model was constructed by assuming an analogy between the unsteady gradient diffusion process and the transport of turbulent kinetic energy by the fluctuations. An empirical error function least squares curve fit, a diffusional power law and diffusion coefficients were derived. The empirical coefficients of self-diffusion were found to be 10·4 and 68·6 $cm^2\ s^{-1}$ for the longitudinal and transverse turbulent energy components, or about a hundred and five hundred times faster than molecular viscous shear diffusion, respectively. This self-diffusion mechanism by microscale size eddies may account for some of the error found by other investigators in balancing the measured terms of the turbulent kinetic-energy equation.

1. Introduction

There exists a need for experiments designed specifically to determine the interaction characteristics of various terms in the turbulence equations. The two-dimensional, incompressible, uniform-density mixing layer is one of the simplest non-homogeneous shear flows. Ideally, the mixing occurs between two uniform, perfectly smooth, semi-infinite streams, with zero angle of incidence, initially separated from each other by an infinitesimal divider with no boundary layers. The mixing region then propagates into both mean streams. This hypothetical two-stream mixing flow has been approximated in several ways in earlier studies for a variety of mean flow velocity ratios. These include, for example, the works of Liepmann & Laufer (1949), Baker, Tao & Weinstein (1970), Wygnanski & Fiedler (1970) and Spencer & Jones (1971).

There is one major characteristic common to these earlier works. They were concerned primarily with the turbulence energy generation in the mean shear region at the interface between the fluid streams. They reasoned correctly that the overall turbulence structure of a mixing layer is governed by its large scale effects. The more

0022-1120/80/4533-2060 $02.00

delicate turbulent characteristics of turbulent energy mixing were totally dominated by the shear generated turbulent structure so as to be undetectable in these traditional turbulent shear flow experiments.

To examine these turbulent mixing quantities, a unique flow geometry had to be configured. A flow had to be maintained that has essentially no mean velocity difference but possess different characteristic and identifiable turbulent structures. This was achieved by using a parallel rectangular bar grid turbulence generator. The bar spacing in each half of the grid was adjusted to produce two initially parallel flowing streams that exhibited the same mean flow structures but possessed significantly different turbulent characteristics. These differences were distinguished by their individual turbulent kinetic energies and associated length scales.

Transport of turbulent energy is by two modes. The large-scale motions transport by simple convection of fluid packets while there is smaller scale transport by gradient diffusion. In this experiment only the later mechanism is present and so a simple gradient diffusion model could be constructed. By analogy, the self-diffusion coefficients were found to be a hundred and five hundred times ordinary molecular diffusion values for the longitudinal and transverse components respectively. It is not easy to determine how those values compare with mean shear flow diffusion rates. In those self-preserved flows, turbulence energy is generated by the mean shear and must be transferred towards the boundaries at a very quick rate contributing to the mixing layer spread. In some cases, this can be a hundred times the gradient diffusion rate.

This experimental investigation was conducted primarily to gain considerable new information and insight into the turbulent structure and turbulent self-diffusion process. As many of the traditional turbulent models require a mean shear gradient for formulation, these are not applicable to this flow. Therefore, it is not the intention to give credence to any particular theoretical development. Although it is expected that this additional data may be used to modify empirical formulations in existing turbulence models and to provide data in a simplified flow for testing competing models.

2. Experimental apparatus and instrumentation

The experiments were performed in a low speed, low turbulence, blowdown wind tunnel. This open return facility has a cross-sectional test section $46 \times 61 \times 366$ cm long. The test section has three fibreboard sides and one Plexiglas side for viewing. A slight divergence of the test-section side walls compensates for the boundary-layer growth and gives a zero measurable static pressure gradient. Entry for axial and vertical probe traversing of the flow field is through a slot, centred along the top surface of the test section. The probes are supported by a streamline section in the form of a symmetric airfoil.

When there are no grid turbulence manipulators used, the mean velocity profile across the tunnel is uniform to $\pm 0{\cdot}1$ %. The measured variation in the axial direction along the centre-line is $\pm 0{\cdot}9$ %. The maximum tunnel speed is 45 m s^{-1} but experiments performed here were conducted at considerably lower speeds. The free-stream turbulence level u'/U (local mean) is approximately constant in both cross-section and downstream directions at 0·05 %.

The desired turbulent flow field was produced by utilizing a passive grid turbulence generator upstream of the test section. The monoplane grid was constructed with

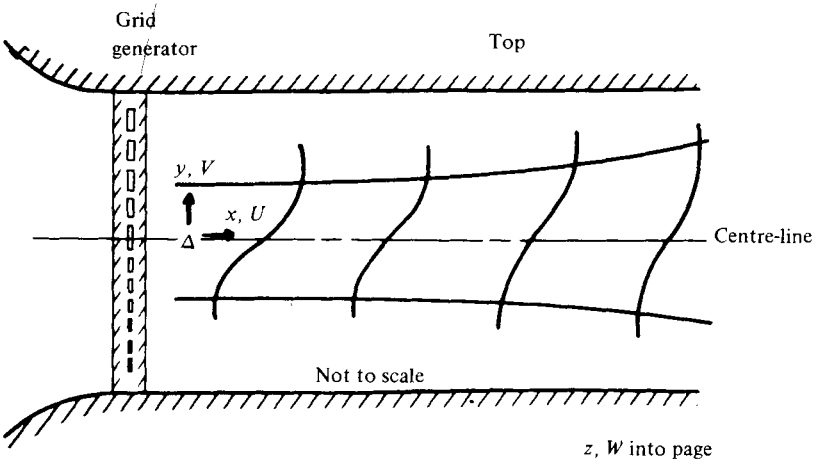

FIGURE 1. Schematic diagram of experimental test section.
△, virtual origin of homogeneous decay.

rectangular parallel bars oriented horizontally with their major axis perpendicular to the flow direction. The uniform mean velocity was achieved by maintaining geometric similarity (solidity) throughout the grid. The difference in the two stream's turbulent intensities was created by requiring the spatial separation between the bars to be twice as large on the top than on the bottom.

The test configuration is shown diagramatically in figure 1 with the co-ordinate system used. The mean velocity profile was set by a tedious trial and error technique of changing the number of bars and local solidity until a uniform profile resulted, to within measuring precision. As the uniform velocity profile was approached, small changes in bar spacing had relatively large non-local effects. The smallest variation in bar spacing was produced by 0·15 mm brass shim stock. The final configuration employed seven $3{\cdot}2 \times 9{\cdot}5$ mm and fifteen $3{\cdot}2 \times 4{\cdot}75$ mm bars with nominal spacings of 19 and 9·5 mm, respectively. The assembly has a static pressure drop solidity of 26·9 %.

As the grid spacing was changed to produce a uniform mean velocity profile, it became very difficult to maintain a 'normal bar' spacing at the boundary. The result was a mean velocity overshoot, or jetting, near the boundary; an effect normally found in grid generated turbulence. It was hypothesized that this was due to the lack of an energy sink on the boundary corresponding to the wake of an adjacent bar, for the energy contained in the jet between bars. Halving the width of the two-dimensional jet adjacent to the walls, thereby approximately halving its energy content, produced a much smoother wall boundary flow.

The primary instrumentation used consists of a pair of a Thermo Systems Model 1054 A constant-temperature hot-wire anemometer used in conjunction with its associated built-in linearizer. The two component fluctuations were simultaneously measured by a symmetric X-array probe specially fabricated for these experiments. The output signals were filtered at 10 kHz to obtain a suitable trade-off between bandwidth and noise. This reduced the electronic noise level from 0·0037 to 0·001 V r.m.s., probably consisting mainly of acoustic noise and mechanical vibration. It is estimated that the mean velocity measurements are accurate to $\pm 0{\cdot}15$ % at typical

velocities. No corrections for finite hot-wire length were applied to the data because for a wire with a length to diameter ratio of order 300, they would have been negligible.

After the X-wire probe outputs were suitably preconditioned and linearized, they were electronically manipulated to produce voltages proportional to the instantaneous longitudinal and transverse velocity components. These signals were recorded on a four channel FM tape recorder at the highest tape transport speed to take advantage of the largest bandwidth. There was no additional filtering in the hot-wire circuit so that the recorded signal was of maximum fidelity.

The analog recording was played back through an analog to digital converter to an IBM 1800 digital computer. The playback speed was one fourth the record speed and the signals were digitized at the maximum real time sampling rate compatible with moving converted data to disk storage for later digital processing. This gives digital signals reproduced faithfully to close to the upper limit frequency response of the recorder. Fourteen bit precision (plus sign) resulted in an amplitude resolution of typically 0·008 f.p.s. or 0·05 % full scale voltage. This was probably greater than was necessary considering the stability of hot wire transducer output. At each position, 38,400 samples were digitized, corresponding to approximately 9·6 s of real time information.

During the tape recording of the data, several primary quantities were monitored, on-line, with the analog instrumentation for comparison and calibration purposes. On completion of each traverse, the first data point was repeated to evaluate instrumentation drift. At the completion of the entire test, the probe was repositioned at the first testing station and the measurements repeated. This procedure yielded excellent reproducibility of the calibration information indicating that the drift effects were nearly indetectable.

Nine sets of data were obtained at representative downstream locations. The first measuring station was located at a position where the statistical fluctuation in measurements of the centre-line turbulent intensities was reduced to a value in line with those obtained at later axial stations. That is, the necessary integration time to provide statistical convergence was on the order of the integral time associated with the turbulence. This choice of first position was consistent with the distance found necessary for the individual bar effects to coalesce in homogeneous grid-generated turbulence.

Each data set is comprised of twenty-five transverse data points spaced in such a way as to sample the mixing region throughout the length of the tunnel but to avoid recording data associated with the boundary layers. Two additional transverses were made at the third downstream measuring station; off centre-line, and with the X-meter probe rotated 90° to measure u and w turbulent components.

At each of the 275 data positions, a complete evaluation of the measurable turbulence characteristics was obtained. The directly measurable quantities were two first moments, three second moments, four third moments, and two fourth moments. Other higher correlations were also computed for comparison with existing measurements to determine the validity of the computational techniques. However, these correlations were not generally determined because of the prohibitive increase in necessary computational time, although good agreement was obtained for those few correlations checked. In addition, at each position two spectra, u'^2 and v'^2, were computed by using a fast Fourier transform. The secondary properties, two dissipative

(Taylor) microscales and two integral scales, and the statistical probability density functions were obtained. The reproduction of all this information here is prohibited by spatial requirements, so only representative data will be presented. A more complete set is given by Gilbert (1975) and Gilbert & Komar (1977).

Several FORTRAN programs were developed and run consecutively to evaluate various turbulent quantities. An important element of the digital computational technique is the fast Fourier transform algorithms. In general, there is excellent correlation between digital and corresponding analog measurements. A comparison of analog to digital techniques has been made by communication engineering users such as Blackman & Tukey (1959) and Bendat & Piersol (1971). The consensus is that while analog methods are quick, they require considerable maintenance and lag behind digital methods in precision and sensitivity.

The data reduction techniques used here are similar to those outlined by Gentleman & Sande (1966) and Van Atta & Chen (1968, 1969). It was shown by Sande (1965) that a 'circular' correlation function is obtained if the procedure is followed without the inclusion of an equal number of 'zeros' to the end of the series in the calculation of the spectra. The effect of this addition is to spread apart the correlation such that 2^n unbiased correlation values are obtained for 2^n data points. Energy spectra calculations were corrected for 'leakage effects'. Calculation of cross-correlations properly accounted for the physical time lag associated with signal multiplexing. The seemingly severe limited frequency response of the digital analysis system does not create any problems in determining turbulent properties because the general features are determined by the large scale components. A minimum of 98·5 % of the total fluctuating energy is reproduced.

3. Results

The mean velocity values were determined from the 'zero frequency' cosine component of a trial fast Fourier transform per set of data corrected by the analog d.c. offset.

The alternative digital technique of summing a great many values and averaging to determine mean values may lead to large errors due to the successively larger truncation of significant figures. This trial value was then used for the augmentation by 'zeros', and the new time series data set was completely analysed. The variation of the centre-line local mean velocity through the test section was 1 %, which provided a check on the wall compensation for boundary layer growth. For an average mean velocity determined by the pressure drop across the contraction, of 14·00 m s^{-1}, the grid Reynolds number was $Re_N = UN/\nu = 1{\cdot}85 \times 10^4$.

The first measurement location was chosen on the basis of the statistical stability of the turbulent mean structure. The flow immediately downstream of the grid reflected the nonuniform nature of the generator. The first measuring station is only 15 normalized mesh lengths downstream which is locally only about 12 large mesh lengths.

In spite of the relatively short flow development length (less than one grid span distance) the mean velocity profile at the first station was quite uniform and statistically stable. The mean velocity profile alone is insufficient to define a fully developed turbulent flow. Generally, the approach towards 'homogeneity' of mean flow is more

rapid than that of the turbulent flow. That is, the turbulent profile is possibly still developing; a situation consistent with observations by Rose (1966) and Champagne, Harris & Corrsin (1970), for turbulent shear flows.

The variation of local mean velocity between successive points was very small, on the order of 0·04 %, which was near the limit of resolution of the instrumentation. This magnitude of mean velocity variation corresponded to a mean shear rate of 0·87 s^{-1}. Assuming a simple Prandtl mixing length model, the turbulent kinetic energy generation from this mean shear would be of the order of 0·13 %. Since grid generated turbulence in this flow for the two levels is initially 6·0 and 4·2 % of the mean, this quantity of mean shear generated turbulent energy is negligible.

To verify two dimensionality the mean velocity profiles were obtained on the centre-line at the third station downstream as measured by the X-probe oriented in the x–y and x–z planes and also obtained off the centre-line of the tunnel. The indication of two-dimensional mean flow is excellent.

The assumption that the cross stream mean velocity component would be essentially zero is verified by the data. The maximum transverse mean velocity component is measured at the first station and has a dimensional value of somewhat less than 0·2 m s^{-1}. This value is reduced to less than 1·5 % by the third measuring station, where it is assumed that the flow was fully developed. There seems to be little indication of the induced transverse mean velocity present in other turbulent mean flow mixing investigations (Spencer & Jones 1971).

There are no second-order effects measured that could be attributed to the presence of a transverse mean velocity component. There are no detectable boundary-layer effects or additional shear generation of turbulence energy due to the existence of transverse mean velocity components.

The mean component turbulent kinetic energies are determined similar to the mean velocity measurements. The average value of the squared component velocity time series is calculated by fast Fourier transform, and monitored by on-line analog instrumentation.

At any cross section, there exists two regions of uniform turbulent energy on either side of the mixing region. These regions associated with large grid spacing and small grid spacing are unaffected by each other, the mixing regions or the wall boundary layers and so behave like ordinary homogeneous turbulent decay flows. These two homogeneous decay curves are shown in figure 2. The third curve shown is the centre-line decay curve. It was not expected that this curve would exhibit a simple decay pattern or possess the same virtual origin as the two non-interactive decay curves because the decay characteristics of the centre-line turbulence were influenced by mixing. However, a linear decay curve was found (as predicted by some multiscale length theories, e.g. Hong 1975) and was assumed to possess the same characteristic decay as the two adjacent, unaffected decay curves. An equivalent characteristic length scale was determined for the centre-line flow. That is, the scale length, N, that would be needed in a uniform grid with the given solidity of 26·9 % to produce a turbulent structure with the same centre-line decay characteristics as the experimental non-uniform grid. The resulting 20·9 mm length corresponded to somewhat less than the overall average mesh spacing.

The virtual origin was found by extrapolating the decay rate curves to their intercepts. The virtue origin for each curve was about 12·8 mesh distances downstream

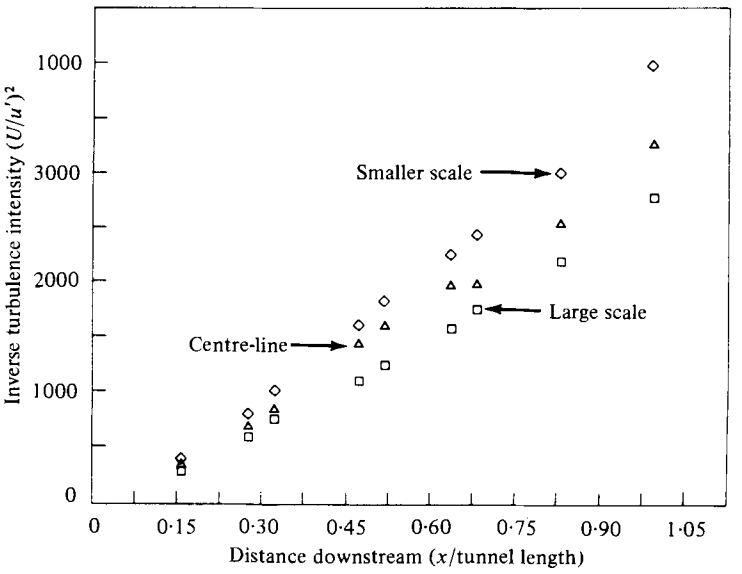

FIGURE 2. Longitudinal turbulent decay at three stations across the flow.

which is consistent with the virtual origin determinations found in most grid turbulence investigations (Corrsin 1963). The two homogeneous decay curves yielded values for their virtual origins which differed by less than 6 mm out of over 340 cm of test length.

The downstream development of the longitudinal turbulent energy component is shown in figure 3. The flow is from bottom to top where the distance between the displaced ordinate origins is proportional to the physical distance between measuring stations. The left side of the graph corresponds to the larger grid spacings. The agreement with on-line measurements is to within less than 1 %. The reproducibility of measurements is an indication that the turbulent component field is well established.

These profiles seem to evolve in a manner very similar to the mean velocity profiles in usual turbulent mixing experiments. However, the turbulent energy mixing mechanism in these two flows is significantly different.

The fluctuating velocity component at each downstream location was curve fit up to the tenth degree polynomial. Uniformly the fifth degree polynomial provided the best least squares fit. However, the traditional analysis of mean shear flows gives an analytical similarity solution for the mean flow in the form of an error function curve. It was found that in all cases, an error function curve fit yielded a superior correlation to the data than did the best polynomial curve fit.

A curve of the functional form

$$u'^2 = A + B\,\mathrm{erf}[\alpha_u(y-\beta)]$$

was used. Unlike the polynomial curve fits, each of the calculated coefficients has easily recognizable physical interpretations: A is the initial large scale, large energy component turbulent intensity level; $B/A = R_u$ is the ratio of the u'^2 component turbulent energy in the unmixed regions; $\alpha_u(x)$ is a coefficient related to the spread rate of the u'^2 in the mixing zone; and β is the centre-line co-ordinate distance from some arbitrarily chosen vertical reference. When the terms α_u and β are prescribed,

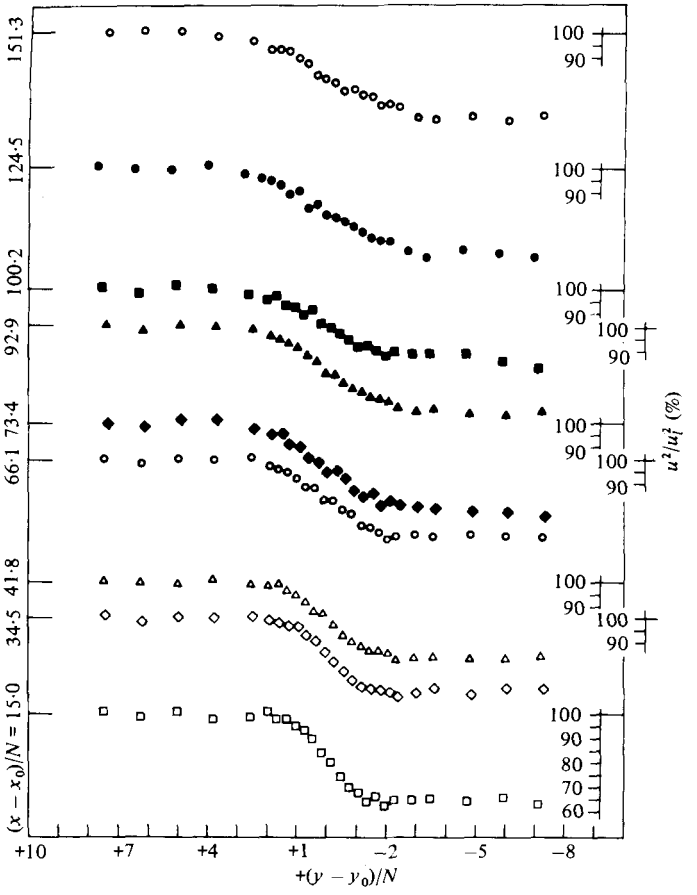

FIGURE 3. Longitudinal component of the turbulent kinetic energy.

the values of A and B are explicitly defined in a linear least squares approximation curve fit sense. The choice of values for α_u and β is based upon a sequential dichotomous search technique used to minimize the standard error of the curve fit.

The profiles given have been normalized with respect to the larger scale component energy as determined by the curve fit, A. The co-ordinate axis has been shifted by applying the centre-line correction, β, and normalized. The variation in β, that is, the wandering of the centre-line co-ordinate of the flow, was only about 0·3 cm along 340 cm of test section. This may be compared to the considerable deflexion of error function curves found in mean flow mixing experiments.

The well-defined mixing-length parameter resulting from the statistical curve fit is used to represent the mixing-layer spread rate as a function of downstream co-ordinate. The spread rate parameter is non-dimensional since the y values were normalized. The spread rate does not have the linear mean flow mixing characteristic exhibited in shear mixing experiments. There is a variation of several percent in the log least squares curve fit determined slopes in several sets of experiments confined between 45 to 63 %.

It is characteristic that two-dimensional similarity turbulent flows develop in the downstream direction as an even root power law. This general nature of turbulent

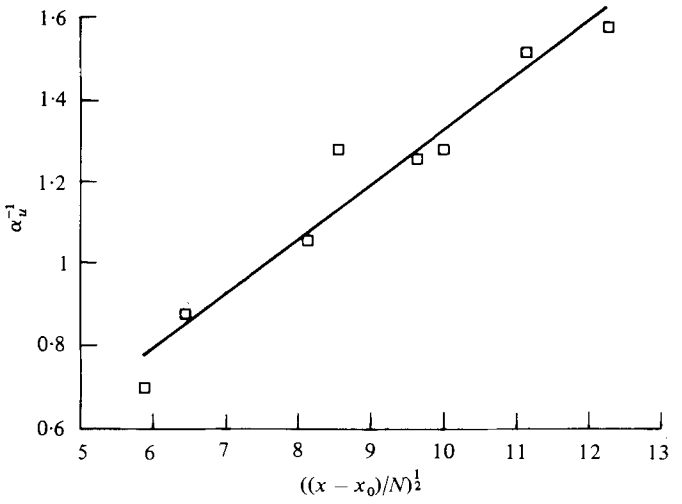

FIGURE 4. One-half power-law curve fit to the non-dimensional longitudinal spread-rate parameter.

flows prompts the choice of $\frac{1}{2}$ power law to be characteristic of the spatial diffusion rate of the mixing region. Envoking Taylor's approximation in this flow where there exists a uniform constant mean velocity, the temporal diffusion of turbulent intensity in the Lagrangian frame also proceeds as time to the $\frac{1}{2}$ power.

Having assumed the form of the spread parameter, α_u, as a $x^{-\frac{1}{2}}$, a new 'similar' variable and non-dimensional spread rate parameter is defined. When both x and y have been normalized and corrected for their respective origins, the decay-rate equation with respect to the large-scale (l) turbulent energy, may be written as

$$\frac{u'^2}{u'^2_l} = 1 + R_u \operatorname{erf} \sigma_u \eta',$$

where σ_u is the constant spread rate parameter,

$$\eta' = y/x^{\frac{1}{2}}$$

and

$$R_u = -0{\cdot}331 \pm 7\ \%.$$

It should be noted that the ratio of the component turbulent energy R_u, remains nearly constant because the decay-rate characteristics of the flows outside the mixing region are similar. Variation of R_u is less than 7 %.

The numerical value of σ_u was found by considering the transformed variables. The inverse of the mixing parameter σ_u is considered associated with the mixing-layer thickness. A plot of this variable versus the normalized downstream co-ordinate to the half power is shown in figure 4 with its linear least-squares curve fit.

Several important features should be pointed out. There is no reason to expect that the virtual origin of the mixing layer would correspond to the origin determined by the homogeneous decay curves. However, extrapolation of the mixing-layer curve indicates the same virtual origin to within 4 mm. This implies that the mechanism involved in the formation of the mixing layer requires a fully developed turbulent structure. That is, while the turbulent flow characteristics are in the transition between the low turbulent level mean flow upstream of the grid, through the individual jet

coalescence, to the final uniform structured turbulent flow, the development of a mixing layer due to the interaction of two streams is not possible.

The existence of truly equilibrium turbulence structures does not exist until at least the second and probably the third measuring location. The existence of individual bars in the turbulence generator is 'remembered' by the flow until this location. Since there exists no simple structure mixing in the upstream region, it would be expected that the mixing zone would not exhibit a structure of the same form as it would downstream, where simple conditions did prevail. That is, the centre-line flow would also remember its discontinuous grid origins for a distance similar to the homogeneous side flows. This hypothesis is supported by the large variation in the mixing parameter, α_u, at the first station. It also further substantiates the contention that the simple turbulent structure did not exist at the first position downstream, although the mean velocity was well behaved. Therefore, since the flow was probably still in a state of adjustment, the first station values were not used in the curve fit.

The spread rate parameter σ_u is found from the curve fit to be 8·36. This value is dimensionless since both x and y are corrected for their respective origins, and are non-dimensionalized by the equivalent mesh spacing, N. The numerical value of σ_u, however, actually is a function of this particular method of non-dimensionalization. The component turbulent velocity similarity parameter, $\eta' = y/x^{\frac{1}{2}}$ has the same form as such mean velocity similarity transformations as boundary layers along a plate and convergent channel flows, $\eta = y(U/\nu x)^{\frac{1}{2}}$. Although the mechanisms are different, this similarity parameter, used with error function profiles, gives a new numerical value to σ_u of 0·0615 when the profile is rewritten in the new functional form

$$\frac{u'^2 - u_s'^2}{u_l'^2 - u_\tau'^2} = 1 - \mathrm{erf}\,(0{\cdot}0615\eta),$$

where the subscripts l and s indicate large- and small-scale structures respectively, for the grid Reynolds number of $Re_N = UN/\nu = 1{\cdot}85 \times 10^4$.

The spread parameter, σ_u, was theoretically a constant and served to correlate the data obtained over the narrow range of Reynolds numbers tested in this experimental facility. Sensitivity to geometry remains wholly untested. Further, the limited range of Reynolds numbers tested does not permit conclusions to be made as to the universality of this constant.

It is interesting to note that the component turbulent kinetic energy seems to diffuse in the longitudinal direction as a one half power. The same diffusion length relationship is found in the definition of dissipation length scales in terms of integral scale lengths, where the latter are directly related to the physical size of the large scale eddies. The indication is that the diffusion of turbulent kinetic energy and the dissipation process may scale in a very similar manner.

Further evidence of this diffusion rate characteristic is found from the diffusion of the lateral turbulent kinetic energy component. Employing many of the previous arguments, a similar error function curve fit was found to give good agreement with the v'^2 turbulent component energy profiles, shown in figure 5. Coefficients of the curve fit have the same physical interpretation as before. The variation in the centre-line of the profile is less than 0·64 mm over the first five locations. At the downstream locations this deviation increases to approximately 2·5 cm in the direction towards the lower energy side of the flow.

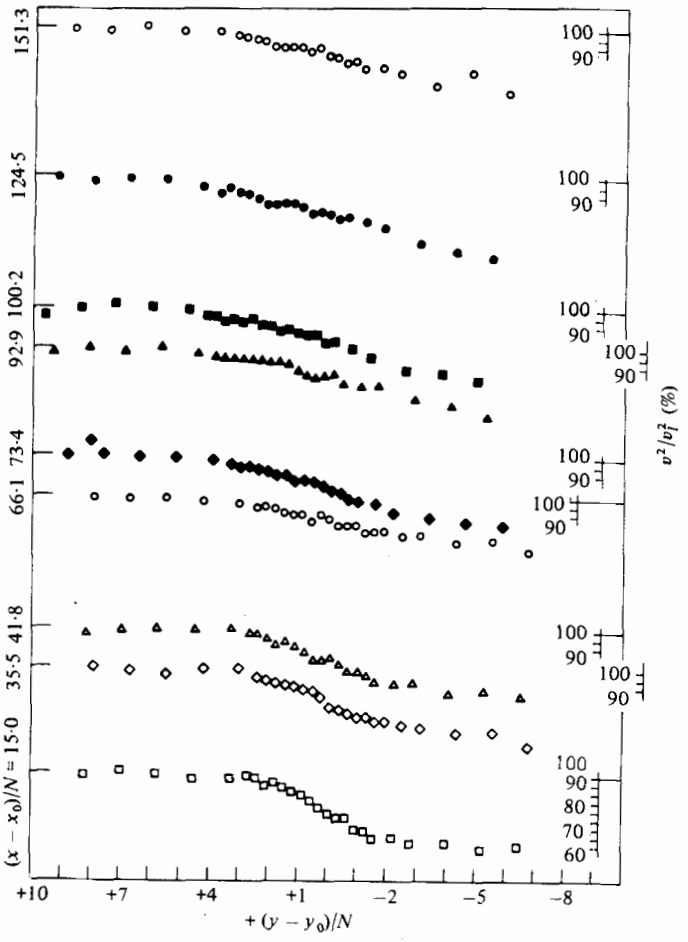

FIGURE 5. Transverse component of the turbulent kinetic energy.

The choice of a $\frac{1}{2}$ power for the spread rate parameter, α_v, was prompted, in part, by the desire to obtain a simple, even root power law relation. The transformed variables, the inverse spread parameter, and the downstream co-ordinate to the minus one half power, are shown plotted in figure 6, together with its linear least squares curve.

The non-dimensional value of the lateral component turbulent energy, α_v, with the particular co-ordinate normalization chosen is 3·27. Maintaining the error function curve fit and introducing again the boundary layer flow type similarity variable $\eta = y(U/\nu x)^{\frac{1}{2}}$, the numerical value of α_v becomes 0·0240 and so

$$\frac{v'^2 - v_s'^2}{v_l'^2 - v_s'} = 1 - \mathrm{erf}\,(0{\cdot}024\eta)$$

where $R_v = -0{\cdot}354 \pm 14\,\%$.

The ratio of the spread rate parameters for the component turbulent energy in the lateral and longitudinal directions is 39·11 %. That is, the lateral component spread in the cross stream direction is 2·56 times as fast as the longitudinal component.

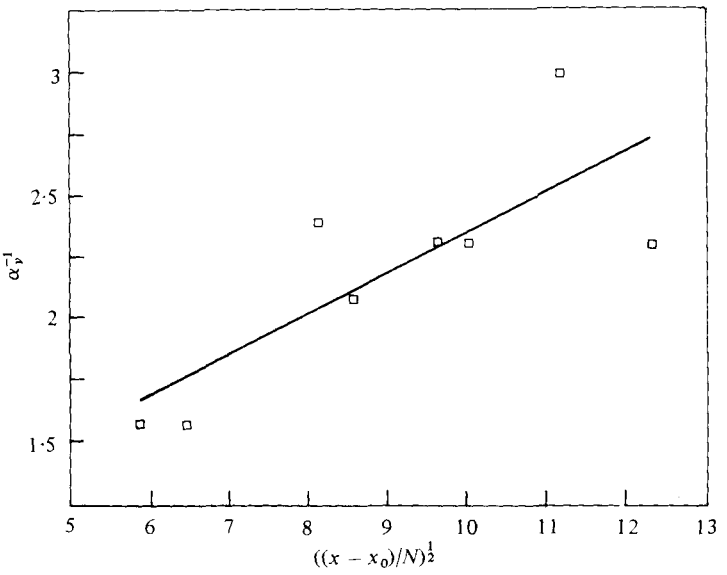

FIGURE 6. One-half power-law curve fit to the transverse non-dimensional spread-rate parameter.

The virtual origin of the component spread rate corresponds to the origin of the homogeneous decay curves to within a negligible amount. The first measuring station results are again exluded in the curve fit. The last station is also not used because of suspected boundary layer interference. The presence of the lower tunnel wall prohibits the further growth of the mixing region, and therefore, the value obtained for the spread parameter is not the same as if the flow had remained a free turbulent mixing flow.

The increased penetration of the v'^2 mixing region leads to the interference of the boundary layer at the last measuring location. A simple calculation of the thickness of the mixing layer for the u'^2 component yields a nondimensional value of 2·42 or about 5 cm off the tunnel's centre-line, allowing more than enough free homogeneous flow region between the mixing and boundary layers. On the other hand, a similar calculation for the v'^2 component turbulent energy gives a non-dimensional distance of 6·19, or about 13 cm half width of the mixing layer. Combined with a slight negative deflexion of the centre-line co-ordinate of the mixing region, there remains less than 7 cm between the end of the mixing region and the wall. The boundary-layer thickness found at this location either via a simple calculation, or direct measurement, is also of this order. The collapse of the component energy profile is due to the interactions between the mixing region and the shear generated turbulent boundary layer flow.

The above analysis of the turbulent profiles is conducted without regard to interactions and redistribution of the turbulent energy between the various components. This is permissible because the nearly isotropic nature of the flow precluded any major net transfer of energy between these components. This is verified by the relatively constant value for the component energy ratios in both cross stream and downstream directions beyond the third measuring station.

Comparisons of longitudinal and lateral turbulent energy profiles measured on and

off the centre-line of the test section at the third station again showed an excellent degree of mean two dimensionality.

The Reynolds stresses were calculated by integrating the co-spectral power density function, determined from the convolution of the individually smoothed, Fourier transformed time series of the longitudinal and lateral component velocities. This technique was employed because simultaneous digital values of the two signals were not available. Multiplexing of the analog to digital converter necessarily produces a small time lag between channel conversions. The lag was measured to be about 40 % of a duty cycle time or about 0·4 ms, real time. A typical f-type temporal correlation coefficient decreased to about 87 % and a g-type to 92 % in this 0·1 ms computer time period. Loss of simple correlation precludes the use of digital multiplication and averaging technique for computing cross correlations. Digital averaging also suffered from truncation error. The spectral computational method is not affected by these factors.

An error comparison was conducted between the on-line measurements and the two digital techniques in a stable region of flow. Digital averaging does not result in asymptotic values. However, for similar integration periods, analog measurements agreed reasonably well with digital fast Fourier transform calculations. There was no basis of determining which method was more correct. In test flows, where the correlation was known, the results agree to within the experimental reproducibility of the measurement.

Based in part upon statistical variations encountered between repetitive measurements of turbulent quantities at a single point in space, a required integration time for measuring any turbulent quantity was determined. Although first, second, and fourth moments converged quite rapidly, the Reynolds stress double correlation at upstream locations requires an inordinate amount of time to satisfy the statistical criterion. At downstream locations beyond the second, reproducibility of the measurements did satisfy the basic criterion. Therefore, from the third station to the last, the major turbulent structure was considered to have lost the memory of the grid generator and to be in a state of local isotropy. The Reynolds shear stress correlation coefficients were all nearly zero, indicating that shear stress played no important role in the redistribution of energy. Measurements of the colateral correlations coefficient $\overline{uw}/u'w'$ never exceed 1 % at the third station. As far as the turbulent structure was concerned, the mean motion is effectively two dimensional.

4. Diffusion analogy

Consider the flow as observed in a frame of reference travelling with the mean flow. The mixing process may be viewed as the simple diffusion of turbulent energy from an area of greater energy content into an area of lesser turbulent energy. It would seem reasonable to define a turbulent energy diffusion coefficient to describe this simple process in such a way as to replace the turbulent diffusion term in the turbulent kinetic-energy equation with an equivalent gradient diffusion term. That is, consider the turbulent kinetic energy as a scalar contaminant which self-diffuses through a uniform continuum field in the transverse direction. This process may then be expressed as an ordinary diffusional mass transfer (or heat conduction) problem, driven by the action of the mean gradient of the scalar property. The longitudinal diffusion of

turbulent energy in the x direction is negligible because the gradient is small. This procedure is analogous to the one followed by Prandtl where turbulent shear stresses are assumed to be expressible in terms of an eddy diffusivity times a mean velocity gradient.

The solution of the one dimensional Fick's (or Fourier's) equation of the form

$$\frac{\partial c}{\partial t} = D_c \frac{d^2 c}{dx^2}$$

with the appropriate boundary conditions, is given by the well-known solution

$$\frac{c - c_f}{c_i - c_f} = 1 - \operatorname{erf}[y/(4D_c t)^{\frac{1}{2}}],$$

where c is any diffusional scalar quantity and the subscripts indicate the initial and final boundary conditions.

Considering the equations of the last section in this form, the constant of self-diffusion of the turbulent energy may be computed by analogy as

$$D_u = 10{\cdot}4 \text{ cm}^2 \text{ s}^{-1}$$

and

$$D_v = 68{\cdot}6 \text{ cm}^2 \text{ s}^{-1}$$

for the longitudinal and transverse turbulent kinetic energy components, respectively, where Taylor's hypothesis has been used. The diffusion was faster than ordinary molecular viscous shear diffusion by factors of about 70 and 460, respectively.

The empirically derived coefficients assumed an analogy between unsteady diffusion (or heat conduction) and the experimental results. This is different than merely assuming transport of a passive contaminant by a turbulent flow field. The latter problem has been examined by other investigators, for example, Skelland (1974).

Direct application of these experimental results may not be proper because the mechanism of transport in the two cases is different. In a gradient diffusion problem, the concentration of the property is assumed to be transmitted by action of molecular motion of particles as they carry the property along with them. In the turbulent transport, the mechanism is associated with small-scale high-intensity turbulent motion as well as large-scale slower motions. If the mean value of the transportable quantity may be considered nearly constant over distances of the order of magnitude of the small-scale structure length, it is reasonable to assume this transport may be described by a gradient diffusion mechanism. The transport by larger-scale motions may be considered purely convective in nature.

The original Taylor's mixing length analogy is an extension of this idea to the transport by packets of fluid being moved under the action of turbulent fluctuations from one location in the field to another. Although this analogy was used to account for the transport of the mean momentum in a mixing region, it may easily be extended to the transport of fluctuation energy, assuming the same mechanism in the absence of generation.

To this extent the analogy is probably reasonable, although it introduces almost all

the objections to Taylor's original theory. Not the least of these is that the turbulent kinetic energy may be transported by the pressure–velocity interaction term in the equation. This term does not have a negligible effect. Even if this term was considered small, no complete analogy may exist between the transport of turbulent energy and the simple mass diffusion (or heat conduction) unless both processes are governed by identical functional forms of the driving force. This does not seem likely.

In spite of these reservations, however, the mechanism of transport seems clear. The large scale motions associated with convective type transport seemed to remain nearly constant. Measurements of the integral scales indicated that the large-scale motions remain essentially unaffected by the cross-stream diffusional process. Therefore, transverse convective transport seemed to be negligible.

However, the mechanism primarily responsible for the cross stream transport of the turbulent kinetic energy is the gradient type diffusion represented by small scale motions. Measurements of the microscale indicated that they are affected by this diffusional process. The integral and microscale measurements for these flows are discussed more completely in Gilbert & Komar (1977).

This result should have been expected. Large-scale motions reflect more of the nature of the flow. For example, the observed trends for energy transport in a round free jet flow is by the large-scale convection motions. The scale size is determined by the mean shear flow and is a significant percent of the total mixing layer width. No simple gradient diffusion is observed, in contradiction to the trends of this experiment. Here, the large-scale dynamics of the flow were characterized by uniform decay as reflected by the large-scale motion. Lack of a convective transport allowed the more subtle nature of gradient diffusion to become apparent. A correct turbulence model should account for the dual structure of transport.

5. Concluding remarks

An experimental examination of fundamental properties of turbulent energy transfer by diffusion in a free turbulent mixing-layer flow has been conducted. Traditional turbulent shear-flow measurements are incapable of determining diffusion mechanisms because of the presence of the dominant mean shear generated turbulence. Two initially parallel flowing streams were produced by using a parallel bar grid which contained the same mean flow structures, but exhibit significantly different turbulence characteristics; specifically, a different turbulent kinetic-energy level.

The mean flow was uniform with only slight variation downstream. There was no apparent induced cross-stream mean velocity such as is evident in mean shear flows. Linear decay curves applied to different parts of the flow all yielded the same virtual origin. Upstream of this virtual origin (about 12·8 mesh diameters), the flow was dominated by the individual jets formed by the grid as they coalesced into a uniform, homogeneous flow. The turbulent diffusion mixing process either did not start before the violent jet mixing process settled down or was so small by comparison that it was undetectable.

The component turbulent-energy profiles showed good correlation with an error function curve fit. A spread rate parameter and centre-line deflexion for the mixing layer was determined. A similarity non-dimensional co-ordinate was introduced and the functional form was determined. Since the functional form is similar to a diffusion

equation, a self-diffusion coefficient was found by analogy for each as

$$D_u = 0{\cdot}00104 \text{ m}^2 \text{ s}^{-1} \quad \text{and} \quad D_v = 0{\cdot}00686 \text{ m}^2 \text{ s}^{-1}.$$

Care must be taken when drawing analogies about turbulent kinetic-energy transfer. Energy transfer may also be through the pressure–velocity correlation mechanism. This term was found, by implication, to be small but not negligible.

An attempt to correlate these experimental results with some well-established results was not fruitful. There are no experimental results for any flow which approximates the unique flow situation developed here. A comparison with at least three theoretical approaches was also attempted. The mean gradient diffusion (Boussinesq) type approach automatically fails because the gradient was zero. The phenomenological differential equations of Spalding (1969) were tried under the assumption that they would simplify enough to be easily solved. However, the resulting set of equations required the development of a computer technique such as Patankar & Spalding's (1970) to be solved. This was outside the scope of this work. The statistical probability approach used by Hong (1975) was examined. Although the kernel used in the probability integration did simplify somewhat, the resulting integral remained nested seven deep. The solution of this equation required prohibitive amounts of computer time and was also beyond the scope of this work.

Further experimental work would be expected to encompass three major areas; examination of the existing flow with an emphasis on extending the Reynolds number range of applicability, examination of the mechanism of combined convectional and diffusional transfer for length scale dependency, and study of the mechanism of turbulent kinetic energy transfer by pressure–velocity correlation.

A future experiment that introduces a scalar contaminant is suggested, for example non-isothermal flow. One stream could be heated with respect to the other and the thermal-diffusion processes examined. This extension would be beneficial to the understanding of the gradient diffusion process, however, requires the development of some additional instrumentation and measuring capabilities. Finally, there should be an effort to establish correlations between experimental results and existing theories. The works of Spalding and Hong are promising in this respect.

This work was conducted at the University at Illinois at Chicago Circle and supported by the Department of Energy Engineering. The author would like to express his gratitude to Dr C. Wolf, Dr J. J. Komar and Dr P. M. Chung for their contributions and support; and to Mr W. Ross and staff for fabrication and design suggestions.

REFERENCES

Baker, R. L., Tao, L. N. & Weinstein, H. 1970 The mixing of two parallel streams of dissimilar fluids. Part I. Analytical development. *A.S.M.E. Paper*, no. 70–WA/APM–37.

Bendat, J. S. & Piersol, A. G. 1971 *Random Data: Analysis and Measurement Procedures.* Wiley.

Blackman, R. B. & Tukey, J. W. 1959 *The Measurement of Power Spectra from the Point of View of Communications Engineering.* Dover.

Champagne, F. H., Harris, V. G. & Corrsin, S. 1970 Experiments on nearly homogeneous turbulent shear flow. *J. Fluid Mech.* **51**, 81.

CORRSIN, S. 1963 Turbulence: experimental methods. In *Handbook der Physiks*, vol. 8, part 2. Springer.

GENTLEMAN, W. M. & SANDE, G. 1966 Fast Fourier Transforms for Fun and Profit. *AFIPS Proc.* 1966 *Fall Joint Computer Conf. Washington, D.C.* 29, p. 563.

GILBERT, B. L. 1975 An experimental investigation of turbulent mixing of fluids with different dynamically significant scales. Ph.D. thesis, Dept. of Energy Engng, University of Illinois, Chicago.

GILBERT, B. L. & KOMAR, J. J. 1977 Turbulent mixing of fluids with different dynamic scales. *Proc. 5th Biennial Symp. on Turbulence, Rolla, Mo.*

HONG, Z. C. 1975 Turbulent chemically reacting flows according to a kinetic theory, Ph.D. thesis, Dept. of Energy Engng, University of Illinois, Chicago.

LIEPMANN, H. W. & LAUFER, J. 1949 Investigation of free turbulent mixing. *N.A.C.A. Tech. Note* 1257.

PATANKAR, S. V. & SPALDING, D. B. 1970 *Heat and Mass Transfer in Boundary Layers*, 2nd edn. London: Intertet.

ROSE, W. G. 1966 Results of an attempt to generate a homogeneous turbulent shear flow. *J. Fluid Mech.* **25**, 97.

SANDE, G. 1965 On an alternative method for calculating covariance functions. *Princeton Computer Memo.* Princeton, New Jersey.

SKELLAND, A. H. P. 1974 *Diffusional Mass Transfer.* Wiley.

SPALDING, D. B. 1969 The calculation of the length scale of turbulence in some shear flows remote from walls. *Prog. Heat Mass Transfer* **2**, 255.

SPENCER, B. & JONES, B. G. 1971 Statistical investigation of pressure and velocity fields in the turbulent two-stream mixing layer. *A.I.A.A. Paper* 71-613.

VAN ATTA, C. W. & CHEN, W. Y. 1968 Correlation measurements in grid turbulence using digital harmonic analysis. *J. Fluid Mech.* **34**, 497.

VAN ATTA, C. W. & CHEN, W. Y. 1969 Measurement of spectral energy transfer in grid turbulence. *J. Fluid Mech.* **38**, 743.

WYGNANSKI, I. & FIEDLER, H. 1970 The two-dimensional mixing region. *J. Fluid Mech.* **41**, 327.